

# Species Specificity of Ectopic Bone Formation Using Periosteum-Derived Mesenchymal Progenitor Cells

JEROEN EYCKMANS and FRANK P. LUYTEN, M.D., Ph.D.

## ABSTRACT

To investigate novel cell-based bone-engineering approaches using rabbit as a preclinical animal model, we compared the osteogenic potential of rabbit periosteum-derived cells (RPDCs) and human periosteum-derived cells (HPDCs) *in vitro* and *in vivo*. Adherent periosteal cells from both species were expanded *in vitro* and subsequently treated with osteogenic medium or bone morphogenetic protein 6 (BMP6). Alkaline phosphatase (ALP) activity was measured, and alizarin red staining was performed to evaluate osteogenic differentiation. *In vivo* ectopic bone formation was assessed by seeding  $5 \times 10^6$  periosteal cells, grown in osteogenic conditions, in a Collagraft carrier and subsequent implantation subcutaneously in athymic mice. *In vitro*, growth analysis indicated that RPDCs expanded faster and were smaller than HPDCs under the same culture conditions. Osteogenic medium did not affect the ALP activity of HPDCs or RPDCs. In contrast, BMP6 stimulated ALP activity in cultured RPDCs and HPDCs but at different rates. *In vivo*, HPDCs gave rise to extensive bone formation, whereas RPDCs failed to make bone. *In vivo*, cell tracking revealed that engraftment and survival of HPDCs and RPDCs after 8 weeks in the implant were limited. Some HPDCs were incorporated into the newly formed bone. RPDCs and HPDCs displayed distinct growth characteristics and osteogenic differentiation capacity *in vitro* and *in vivo* under the culture conditions used. Our data indicate potential limitations of use of the rabbit as a preclinical model for cell-based treatments for bone repair.

## INTRODUCTION

THE USE OF MESENCHYMAL STEM CELLS (MSCs) in combination with a scaffold is a promising approach for repair of skeletal tissues, in particular for bone. There is increasing evidence that MSCs are present in a wide variety of tissues, such as synovium, cartilage, periosteum, muscle, and bone marrow.<sup>1-4</sup> Of these different cell sources, bone marrow-derived cells (BMDCs) are probably the most extensively characterized and are often used for bone repair because of their osteogenic properties *in vitro* and *in vivo*.<sup>5-8</sup> Another promising cell source for bone repair is periosteum. Periosteum is a bilayered membrane attached to the cortical bone that consists of an outer fibrous layer and an inner cambium layer. The cambium layer contains chondrocyte precursors and osteoblast-like cells that are highly active during callus formation.<sup>9-11</sup> It has been sug-

gested that human periosteum-derived cells (HPDCs) maintain their proliferative capacity in elderly individuals and keep their *in vitro* and *in vivo* osteochondral potential regardless of age or passage, making them interesting candidates for bone-engineering applications.<sup>12,13</sup> Additional advantages of using periosteum-derived cells (PDCs) over BMDCs might be the ease of tissue harvesting and isolation of PDCs.<sup>14</sup> PDCs have been used successfully in skeletal engineering; several groups have demonstrated that PDCs harvested from the rib, tibia, or femur can differentiate toward osteogenic or chondrogenic cells, producing bone and cartilage in different animal models.<sup>14-19</sup>

The insights derived from these animal models are important for the development of novel clinical protocols. In general, animal models are used to test medical products or drugs on safety, toxicity, and efficacy before human clinical trials are initiated. The ideal animal model would be the

one that accurately predicts the outcome of a treatment in patients. Unfortunately, the results obtained in animal models do not always correlate with clinical outcomes. For example, the success rate of repairing cartilage defects with autologous cells is higher in rabbits than in goats or humans, possibly because the intrinsic healing capacity of cartilage is superior in rabbits.<sup>20–23</sup> Rabbits are also widely used as a preclinical model for bone repair.<sup>19,24–27</sup> Unfortunately, it remains unclear whether the rabbit model is comparable with the human model for bone-engineering applications.

To evaluate novel bone-engineering approaches with rabbit as a preclinical animal model, we compared the osteogenic capacity of rabbit periosteum-derived cells (RPDCs) and HPDCs and found striking differences in biological behavior *in vitro* and *in vivo*.

## MATERIALS AND METHODS

### *Harvest of periosteal tissue and isolation of the cells*

Periosteal biopsies (10×5 mm<sup>2</sup>) were harvested from the medial side of the proximal tibia of female adolescent and adult (11, 27, or 34 weeks) White New Zealand rabbits. The periosteum was stripped off the tibia using a periosteal lifter. The periosteal specimens were transported in growth medium consisting of high-glucose Dulbecco's modified Eagle's medium (DMEM, Invitrogen, Merelbeke, Belgium) supplemented with 10% fetal bovine serum (FBS, Bio-Whittaker, Verviers, Belgium) and 1X antibiotic-antimycotic solution (100 units/mL penicillin, 100 µg/mL streptomycin, and 0.25 µg/mL amphotericin B; Invitrogen). The biopsies were finely minced and digested overnight at 37°C in 0.2% crude type IV collagenase (Invitrogen) in growth medium as described above. Subsequently periosteal cells were collected using centrifugation, the supernatant was removed, and the cells were resuspended in growth medium, plated in a T25 culture flask, and allowed to attach for 5 days. Non-adherent cells were removed by changing the medium. Periosteal biopsies of 3 young female human donors (age 15, 21, and 26) were retrieved from the proximal tibia within 6 hours post-mortem and processed as described above.

### *Cell culture*

Cells were expanded in monolayer in growth medium. Upon confluence, PDCs were trypsin released (0.25% trypsin, 1mM ethylenediaminetetraacetic acid; Invitrogen) and replated with a seeding density varying between 10,000 and 15,000 cells/cm<sup>2</sup>. For cryopreservation, PDCs were suspended in DMEM with 20% FBS and 10% dimethyl sulfoxide (Sigma, Bornem, Belgium) and stored in liquid nitrogen. For the *in vitro* and *in vivo* osteogenic assays, cells were thawed, replated, and expanded in T175 flasks (Greiner, Wommel, Belgium). Growth curves were obtained by seeding passage 3 (P3) periosteal cells in 6-well

plates at a cell density of 10,000 cells/cm<sup>2</sup>. Cells were trypsin-released and counted in a Neubauer chamber at day 1, 2, 3, 5, and 7.

### *Evaluation of cell size*

To determine the cell size of PDCs seeded on plastic, RPDCs and HPDCs of young donors (11 weeks and 15 years, respectively) were cultured in 24-well plates for 3 and 7 days, respectively, to obtain comparable cell numbers. After fixation of the cells in 4% formaldehyde, cells were washed in PBS, and excess of aldehyde was quenched with 10 mM ethanol-amine (Sigma). Cytoskeleton was stained with a 1/100 dilution of Cy2-conjugated phalloidin antibody (Sigma) in PBS with 0.2% TritonX-100 for 15 min. Nuclei were counterstained with 4',6-diamidino-2-phenylindole. Fluorescent pictures were taken using a SPOT CCD camera (Diagnostic Instruments, Sterling Heights, MI), and the cell surface area was measured digitally using ImageJ software (National Institutes of Health, Bethesda, MD, <http://rsb.info.nih.gov/ij/>, 1997–2004). More than 120 single HPDCs and RPDCs were divided into 5 categories according to their cell size.

To analyze the cell size in suspension, 3×10<sup>5</sup> HPDCs and RPDCs were trypsin-released and suspended in PBS with 2% FBS. Forward/sideward scatter (FSC/SSC) was measured using a FACSORT machine (Becton and Dickinson, Erembodegem, Belgium). The gates were set in the linear range of the FSC/SSC to reject the small particles and big cell clusters in the measurements.

### *In vitro osteogenic assays*

P3 RPDCs and HPDCs were seeded at 10,000 cells/cm<sup>2</sup> in 24-well plates. After 24 h in culture, the medium was replaced using osteogenic medium [growth medium supplemented with 100 nM dexamethasone, 10 mM beta-glycerophosphate, and 50 µM ascorbic acid 2-sulfate (Sigma)] for 3 weeks<sup>28</sup> or with DMEM medium supplemented with 3% FBS, 1X antibiotic-antimycotic solution, and human recombinant bone morphogenetic protein 6 (BMP6) at 100 ng/mL. The cells were lysed in 150 µL PBS containing 0.05% Triton X 100 (Sigma) at day 3, 9, or 15 and frozen at –80°C until all the samples were collected for further processing. Alkaline phosphatase activity was measured using a commercially available kit (Kirkegaard & Perry, Guilford, UK), according to the manufacturer's instructions. Deoxyribonucleic acid (DNA) content was determined using the Fluorescent DNA Quantitation Kit (BIO-Rad, Veenendaal, the Netherlands). After 3 weeks of treatment with osteogenic medium, calcium deposits were stained using alizarin red. Primary human BMDCs were used as positive controls.

### *In vivo osteogenesis*

P3 PDCs were treated with growth medium, osteogenic medium, or 100 ng/mL BMP6 for 3 days. Subsequently,

PDCs were seeded into Collagraft (Neucoll, Cambell, CA) and implanted subcutaneously in NMRI-*nu* mice (female, 8 weeks) as described previously.<sup>16</sup> Briefly, 5 million viable P3 RPDCs and HPDCs were collected, centrifuged, and suspended in 50  $\mu$ L DMEM with 1% FBS. Collagraft was punched into 21 mm<sup>3</sup> cylindrical (diameter 3 mm, height 3 mm) scaffolds, and 50  $\mu$ L of cell suspension was put on top of each scaffold. To allow cell attachment, the seeded scaffolds were incubated at 37°C for 2 to 4 h. After incubation, the Collagraft was directly implanted subcutaneously on the back in the cervical region of NMRI-*nu* mice. The remaining cells in the supernatant were counted to estimate the seeding efficiency, which was calculated as follows: [(number of seeded cells – number of cells in the supernatant)/number of seeded cells]  $\times$  100. Cell viability was assessed using trypan blue exclusion test. The implants were collected after 1, 4, and 8 weeks of implantation. Half of each implant was fixed in 4% formaldehyde, decalcified in DECAL overnight (Omnilabo, Breda, the Netherlands), paraffin embedded, and processed for histology. The other half was lysed in PBS with 0.05% Triton X 100, homogenized and stored at –80°C until further processing for alkaline phosphatase activity measurements, or suspended in a lysis buffer and used for ribonucleic acid (RNA) extraction as described below. To track the engrafted cells, HPDCs and RPDCs were transduced using an adenoviral vector encoding for green fluorescent protein (GFP, ad-GFP, a gift from Dr. P. Tylzanowski) 24 h before seeding (multiplicity of infection = 130, transduction efficiency ~35%). Detection of the GFP-positive cells in the explants was done using immunohistochemistry with a rabbit anti-GFP polyclonal primary antibody (Abcam, Cambridge, UK) at a dilution of 1:100 and a peroxidase-conjugated goat anti-rabbit secondary antibody (Jackson Immuno-research Laboratories, De Pinte, Belgium) diluted 1:200 and 3,3'-diaminobenzidine (Sigma) as a chromogenic substrate. The sections were counterstained with hematoxylin. For quantification of the engrafted cells, GFP-positive cells were counted in at least 15 sections of triplicate implants. To quantify the amount of bone in the implants, histomorphometry was performed in at least 10 sections per implant, as described by Martin *et al.*<sup>29</sup> Immunohistochemistry for human osteocalcin was performed as described above. The primary antibody against human osteocalcin was a generous gift from Dr. E. Van Herck. The antibody was raised in guinea pigs and does not cross-react with mouse or rabbit osteocalcin.

The local ethical committee approved all procedures related to harvesting periosteal flaps and animal experiments.

#### *RNA isolation and conventional polymerase chain reaction*

Half of the Collagraft was put in a lysis buffer delivered with an RNA extraction kit (Nucleospin, BD Biosciences, Erembodegem, Belgium) and homogenized (Ingenieurbüro

CAT M. Zipperer GmbH, Staufen, Germany). RNA extraction was performed according to the manufacturer's recommendations. Complementary DNA (cDNA) was obtained using reverse transcription of 1  $\mu$ g of total RNA with Oligo (dT)20 as primer (Superscript III; Invitrogen). Conventional polymerase chain reaction (PCR) was performed in 10  $\mu$ L in a PerkinElmer Gene Amp PCR system 9600 (Applied Biosystems, Lennik, Belgium) according to standard procedures. Primer sequences for specific human beta actin have been previously published.<sup>30</sup> Rabbit-specific beta-actin primers were designed in Vector NTI (Invitrogen) based on 2 sequences available on the gene bank (entry: 3': AF309819; 5': AF000313). The sense primer is 3'-GAGAAGCTGTGCTACGTGGCG-5'; the anti-sense primer is 3'-CATGATCGAGTTGAAGGTGGTCTCG-5'.

#### *Statistical analysis*

Data are expressed as means  $\pm$  standard deviations. Statistical significance was determined using a Mann-Whitney U test to compare means between the groups, with a *p*-value less than 0.05 considered to be significant.

## RESULTS

### *Characterization of cell cultures*

To demonstrate morphological differences between RPDCs and HPDCs in cell culture, we took pictures of P3 cells at low density (Fig. 1A, B) and at subconfluence (Fig. 1C, D). Different subpopulations can be distinguished based on morphology. Most of the HPDCs were large, elongated, fibroblast-like cells (Fig. 1A, C), whereas most of the RPDCs consisted of small rectangular, triangular, and spindle-shaped cells (Fig. 1B, D). In both cell cultures, a small fraction of large "pancake"-shaped cells was observed (inset of Fig. 1B). Growth curves (Fig. 1E) indicate that RPDCs proliferated faster than HPDCs and that the cell density of RPDCs was about 3 times as high as that of HPDCs at confluence (day 7). F-actin cytoskeletal staining with phalloidin showed that HPDCs remained in monolayer, whereas the RPDCs grew in multilayers at full confluence (Fig. 1F, G).

To evaluate the physical appearance of the PDCs in cell culture, cell size was measured, and the cell populations were distributed into 5 groups according to their cell size. Sixty-five percent of the RPDCs, but only 6% of the HPDCs, were smaller than 2000  $\mu$ m<sup>2</sup>. The fraction of very large "pancake"-shaped cells (>8000  $\mu$ m<sup>2</sup>) was comparable between the 2 cell types (Fig. 2A). To exclude the effect of cell spreading on cell size, PDCs were released and kept in suspension, and cell size was analyzed using fluorescence-activated cell sorting. FSC is directly related to cell size. Also, in this experiment, a large subpopulation of small RPDCs (35%) was identified (Fig. 2B).

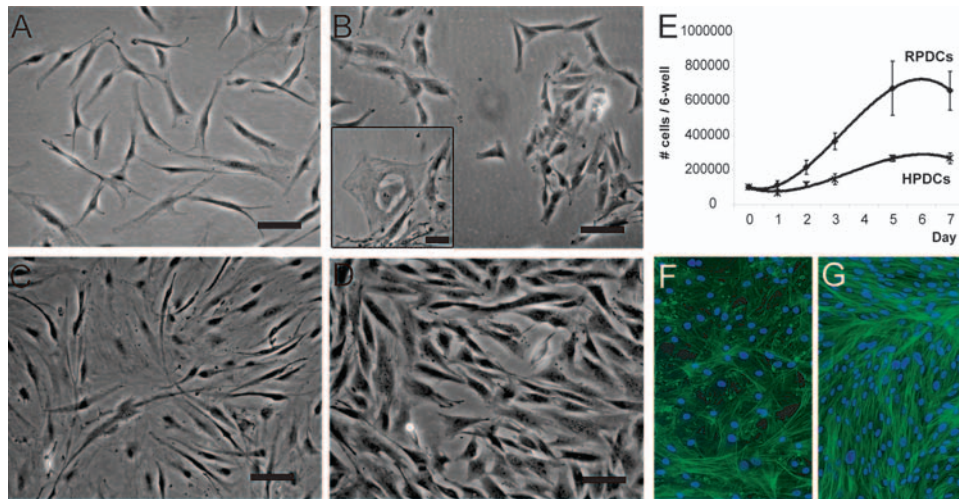


**FIG. 1.** Morphology and growth characteristics of HPDCs and RPDCs. Phase-contrast light microscopy of HPDCs (A and C) and RPDCs (B and D) at low density (A and B) and subconfluence (C and D) (20 $\times$ ; bar: 50  $\mu$ m) shows that HPDCs (A and C) appear to have a more fibroblastic morphology than RPDCs (B and D). In both cell cultures, a subpopulation of large “pancake”-shaped cells was observed (inset of 1B). (E) Growth curve of RPDCs and HPDCs cultured in 6-well plates. (F and G) Cytoskeletal staining of HPDCs and RPDCs, respectively, with a phalloidin antibody showing a multilayer culture for RPDCs at full confluence. The nuclei are stained with 4',6-diamidino-2-phenylindole (blue). Color images available online at [www.liebertpub.com/ten](http://www.liebertpub.com/ten).

### In vitro osteogenesis

To investigate the *in vitro* osteogenic capacity of RPDCs and HPDCs, both cell types were cultured in osteogenic medium or in medium supplemented with BMP6. Several groups have demonstrated that osteogenic medium induces a molecular cascade of events directing the progenitor cells toward osteoblasts.<sup>7,28,31,32</sup> In contrast to human BMDCs, treatment with osteogenic medium did not induce significant increase of alkaline phosphatase activity in HPDCs or RPDCs (Fig. 3A). After 18 days, alizarin red staining revealed stronger mineralization of the HPDCs treated with osteogenic medium than of the RPDCs under identical experimental conditions (Fig. 3C).

To test the alkaline phosphatase (ALP) response of the PDCs in other cell culture conditions, we treated the cells with BMP6, a growth factor known to promote osteogenesis *in vitro* and *in vivo*.<sup>33,34</sup> A dose-response experiment showed that a concentration of 100 ng/mL of BMP6 was optimal to induce ALP activity in RPDCs and HPDCs (data not shown). RPDCs had a more pronounced response to BMP6 than HPDCs (8-fold increase versus 3-fold increase), with different dynamics (Fig. 3B). The highest ALP activity of RPDCs induced by BMP6 occurred at day 3, whereas for the HPDCs the induction of ALP activity started at day 15. In addition, RPDCs from 27-week-old rabbits responded in a similar manner to the RPDCs from 11-week-old rabbits *in vitro* but with delayed dynamics (data not shown). After 18 days of BMP6 treatment, RPDCs but not HPDCs showed alizarin red-positive calcium deposits, confirming the BMP6-induced cascade of osteogenic differentiation terminating in the formation of

calcified nodules (Fig. 3C). The results of these experiments were reproducible in 4 other experiments.

### In vivo osteogenesis

To address the *in vivo* bone formation capacity of the periosteum-derived progenitor cells, HPDCs and RPDCs were seeded in Collagraft (a collagen type I, hydroxyapatite and tricalciumphosphate scaffold) and implanted subcutaneously on the back of NMRI-*nu* mice. The seeding efficiency for the HPDCs was 66%  $\pm$  13%, and that for RPDCs was 51%  $\pm$  19%. Cell viability was estimated at 87%  $\pm$  11% for the HPDCs and 64%  $\pm$  23% for the RPDCs. To exclude possible differences in outcome due to age, we included HPDCs from skeletally immature donors (3 and 10 years old) and RPDCs from skeletally mature rabbits (27 and 34 weeks old) in this set of experiments.

After 8 weeks of implantation, the Collagraft implant seeded with HPDCs showed *de novo* bone formation, whereas the Collagraft implant seeded with RPDCs did not (Fig. 4A, B). Autofluorescent images of the hematoxylin and eosin stainings (Fig. 4B, C) were used to quantify the amount of bone in the implants (Fig. 4D).<sup>29</sup> The implants were filled with an average of 15% (standard error  $\pm$  4%) bone.

No collagen type II or X messenger RNA (mRNA) was detected using Taqman PCR at week 1, 4, or 8 (data not shown).

The lack of ALP activity in the implants at 8 weeks also reflected the absence of *in vivo* bone formation in Collagraft seeded with RPDCs (Fig. 4E). In addition, pretreatment of the RPDCs with osteogenic medium or BMP6

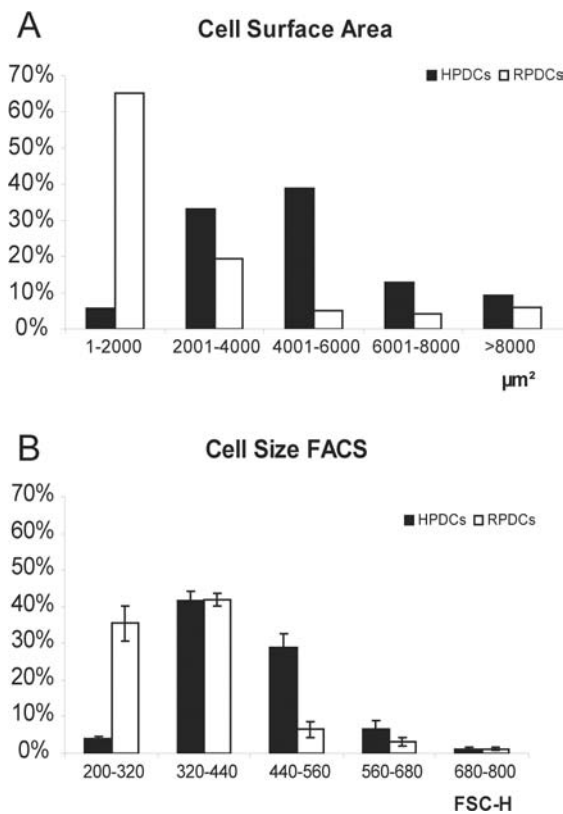


**FIG. 2.** Characterization of the cell size of human periosteum-derived cells (HPDCs) and rabbit periosteum-derived cells (RPDCs). **(A)** Distribution of HPDCs and RPDCs based on the cell spreading area when spread on plastic as measured digitally using ImageJ based on phalloidin cytoskeletal staining. **(B)** Distribution of HPDCs and RPDCs in suspension based on forward scatter (FSC) as obtained using fluorescence-activated cell sorting (FACS) analysis.

before implantation did not induce ALP activity in the implants at 8 weeks. Histological analysis of these implants confirmed the absence of bone (data not shown).

To allow cell tracking, we transduced RPDCs and HPDCs with ad-GFP. In RPDC- and HPDC-seeded scaffolds, GFP-positive cells were found at 1 and 4 weeks post-implantation (Fig. 5A, B, D, E). After 8 weeks, some GFP-positive RPDCs were seen in the explants but few HPDCs (Fig. 5C, F). Quantification of GFP-positive cells indicates a fast decrease of the number of RPDCs after implantation (Fig. 5G). At 1 week, an average of  $110 \pm 48$  HPDCs versus  $59 \pm 18$  RPDCs per section was counted. At 4 weeks,  $87 \pm 18$  HPDCs versus  $9 \pm 2$  RPDCs and at 8 weeks, few GFP-positive HPDCs or RPDCs were observed. Although GFP staining barely detected HPDCs, human-specific beta actin was amplified with conventional PCR (28 cycles) (Fig. 5H). Immunohistochemistry for human osteocalcin revealed positive cells located in or adjacent to bone spicules (Fig. 5I), suggesting that a subpopulation of the implanted HPDCs partially contributed to the ectopic bone formation in Collagraft. Mouse bone was used as a

control for antibody specificity and did not show positive cells (data not shown).

## DISCUSSION

Animal models are widely used in bone engineering to investigate the potency and safety of tissue-engineered products *in vivo*. To create bone-engineered constructs, a wide variety of biomaterials combined with cells derived from diverse tissues and different animals have been used.<sup>24–26,35–37</sup> The results indicate that the combination of cells with an appropriate scaffold may lead to enhanced bone repair *in vivo*. However, there is large variability in the results in preclinical animal models that do not always predict the clinical outcome.<sup>38</sup>

An attractive animal model to test bone-engineering products is the rabbit. Rabbits allow for the creation of much larger critical-size bone defects than mice and rats, and housing costs are more reasonable than for larger animals such as dogs and goats. Unfortunately, not much is known about potential species differences between rabbit and human, which may have implications for the translation of preclinical studies in animals to clinical applications in human.

In an attempt to investigate the potential use of rabbit progenitor cells in preclinical bone-engineering applications, we compared HPDCs and RPDCs *in vitro* and *in vivo*. In cell culture, we have shown that RPDCs grew faster and reached higher cell density than HPDCs when confluent. That the population RPDCs contained a larger subpopulation of small cells that grew in multilayer when confluent could explain this. The presence of small high-proliferative cells could suggest the presence of higher numbers of stem cells. Small cells have been associated with quiescent stem cells in the pancreas<sup>39</sup> but also with rapid self-renewal multipotent progenitor cells in bone marrow.<sup>40,41</sup> In contrast, both cell populations also contain a fraction of large “pancake”-shaped cells that may be originating from the cambium layer.<sup>42</sup>

Therefore, it has been suggested that selection of cells based on cell size results in a more homogeneous cell population displaying stem cell properties.<sup>43,44</sup> Because it has been known for decades that cell size is not directly linked to the size of animals,<sup>45</sup> we hypothesized that the observed subpopulation of small RPDCs was in an earlier stage of differentiation than the HPDCs, because the RPDCs originated from young, growing rabbits. Therefore, we decided to pretreat the cells and enhance their commitment to the osteogenic lineage by adding dexamethasone,  $\beta$ -glycerophosphate, and ascorbic acid to the culture medium. Dexamethasone can induce osteogenic differentiation in bone marrow-derived MSCs derived from different species such as rat,<sup>46</sup> rabbit,<sup>47</sup> dog,<sup>48</sup> and human.<sup>28</sup> In our experiments, addition of dexamethasone did not significantly increase the ALP activity of HPDCs and RPDCs. Alizarin red staining revealed mineralization of HPDCs but

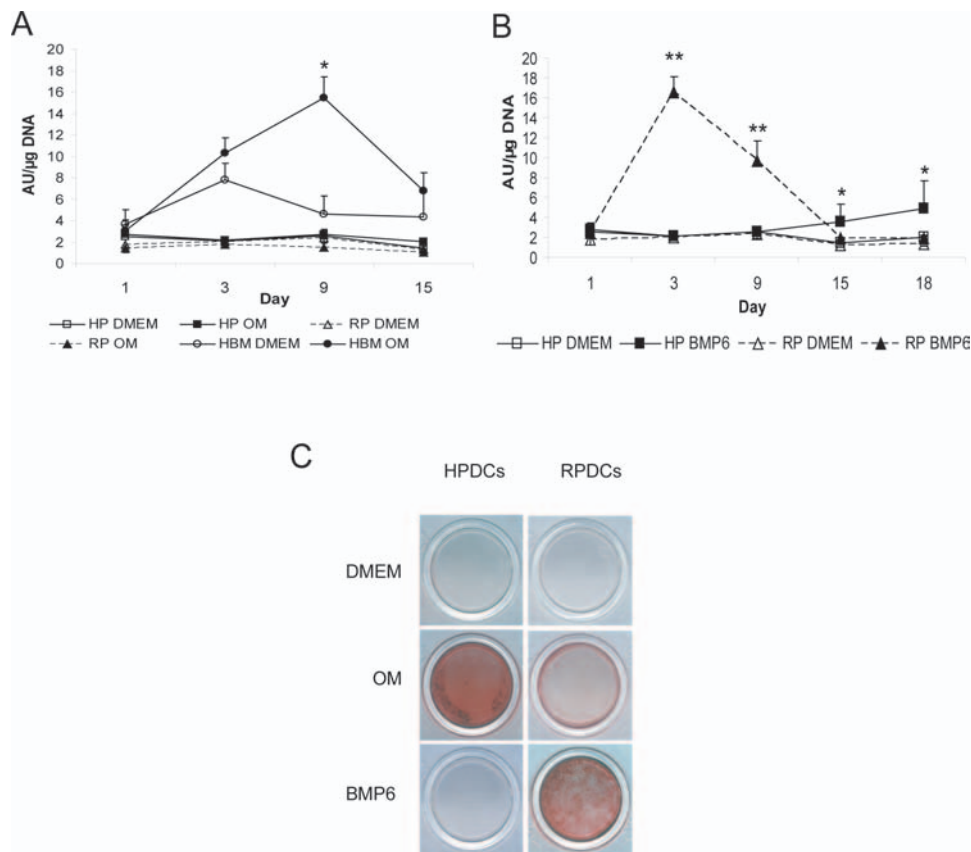


**FIG. 3.** *In vitro* osteogenesis experiment with cells from 2 independent donors. Human periosteum-derived cells (HPDCs) and rabbit periosteum-derived cells (RPDCs) cultured in 24-well plates were treated with osteogenic medium (OM) (A) or 100 ng/mL bone morphogenetic protein (BMP)6 (B). Alkaline phosphatase activity was measured at days 1, 3, 9, and 15. Alkaline phosphatase activity is expressed in absorbance units measured at 620 nm normalized to deoxyribonucleic acid content in  $\mu\text{g}$ . The results of this experiment were reproducible in 5 other experiments (bar = standard deviation;  $*p \leq 0.05$ ,  $**p \leq 0.01$ ). To visualize mineralization, HPDC and RPDC cultures were stained using alizerin red after 18 days of treatment (C). DMEM, Dulbecco's modified Eagle's medium; HBM, human bone marrow; DNA = deoxyribonucleic acid. Color images available online at [www.liebertpub.com/ten](http://www.liebertpub.com/ten).

not RPDCs after 3 weeks of culture in osteogenic medium. Because osteogenic medium did not increase the alkaline phosphatase activity of HPDCs and no osteocalcin mRNA was detected with conventional PCR (data not shown), we assume that the mineralization was of dystrophic origin and was not associated with osteogenesis. As for the RPDCs, our results confirmed the data as reported by Solchaga *et al.*,<sup>49</sup> who also found that osteogenic medium did not induce ALP activity in RPDCs. In contrast, it has been shown that dexamethasone can induce ALP activity in PDCs derived from chickens.<sup>50</sup> The use of different serum batches can explain this discrepancy.<sup>31</sup> We have tested osteogenic medium made with 10 different serum batches, but differences were discrete in cell proliferation or ALP response of PDCs to osteogenic medium.

Because osteogenic medium failed to induce ALP activity in the PDC cultures, we added human recombinant BMP6. BMP6 is reported to be a strong bone inducer *in vitro* and *in vivo*.<sup>33,34</sup> Liu *et al.* reported that dexamethasone can regulate BMP6 mRNA transcription in hu-

man MSCs.<sup>51</sup> Whereas dexamethasone did not induce ALP activity in PDCs in our experiments, treatment with BMP6 increases the ALP activity in human and rabbit PDCs. The ALP response of the RPDCs to BMP6 was more pronounced at day 3 than that of the HPDCs. BMP treatment on human cells in culture is less efficient than on animal cells, especially under serum-containing conditions.<sup>52,53</sup> It has been postulated that BMP-induced osteogenesis *in vitro* of human MSCs is dependent on the presence or absence of serum. In the presence of serum, high extracellular signal-regulated kinase activity down-regulates the BMP-mediated SMAD activity, whereas in the absence of serum, osteogenic differentiation is achieved through p38 and PI3-K/AKT activities.<sup>54</sup> Although we treated HPDCs with BMP6 in low serum conditions, we obtained a more moderate ALP response of HPDCs on BMP6 than with RPDCs.

To test the *in vivo* osteogenic capacity of the PDCs, we seeded the cells in Collagraft and implanted them subcutaneously in nude mice. Several other groups have

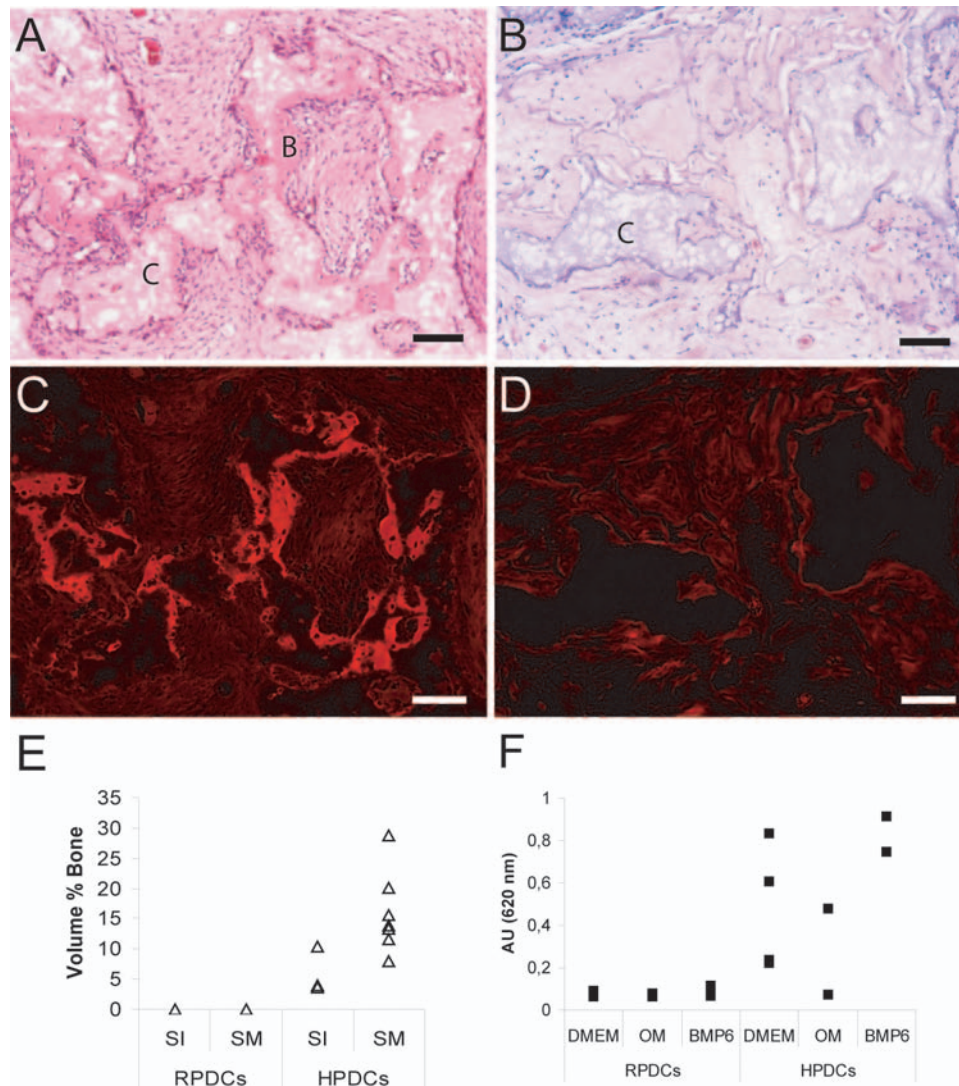


**FIG. 4.** Hematoxylin/eosin staining on a section of Collagraft seeded with human periosteum-derived cells (HPDCs) (A) or rabbit periosteum-derived cells (RPDCs) (B) implanted subcutaneously for 8 weeks in nude mice (B = bone; C = Collagraft; magnification 100 $\times$ ; bar = 100  $\mu$ m). (C and D) Autofluorescent image of panels A and B, respectively. The bright red spots in panel C are bone spicules. (E) Quantification of the amount of bone on 27 implants [skeletally immature (SI) RPDCs:  $n=6$ , skeletally mature (SM) RPDCs:  $n=8$ , SI HPDCs:  $n=4$ , SM HPDCs:  $n=9$ ; each triangle represents 1 implant]. The average percentage of bone volume is estimated on 10 to 25 sections per implant. (F) Alkaline phosphatase (ALP) activity in Collagraft seeded with treated [osteogenic medium (OM) or bone morphogenetic protein (BMP6)] or non-treated periosteum-derived cells (PDCs) after 8 weeks of implantation in nude mice. The ALP activity is expressed in absorbance units (AUs) measured at 620 nm. BMP6; bone morphogenetic protein 6; DMEM, Dulbecco's modified Eagle's medium.

previously used this ectopic bone formation model.<sup>2,16,36,55</sup> We used Collagraft as a carrier because it contains collagen type I, hydroxyapatite, and tri-calcium phosphate, 3 components of bone matrix. Bone mimicking carriers have been used successfully in the regeneration of bone defects.<sup>56–58</sup> In HPDC-seeded implants, bone formation started 4 weeks after implantation and was consistently and reproducibly observed for all donors tested, whereas no bone was formed in the Collagraft scaffolds seeded with RPDCs. The ectopic bone formation activity was independent of the donor age of the seeded PDCs. In an attempt to induce ectopic bone

formation with RPDCs, we pretreated the cells with osteogenic medium or with BMP6 before implantation. Although BMP6 induced the ALP activity *in vitro*, no ectopic bone formation was seen in RPDC-seeded carrier structures. So far, pretreatment with osteogenic medium or BMP6 did not affect the outcome of ectopic bone formation *in vivo*.

Therefore, we hypothesized that the RPDCs did not survive and persist in the scaffolds *in vivo*. Indeed, based on the quantification of the GFP-positive cells, we estimated that only 0.5% of the seeded RPDCs, versus 5% of the

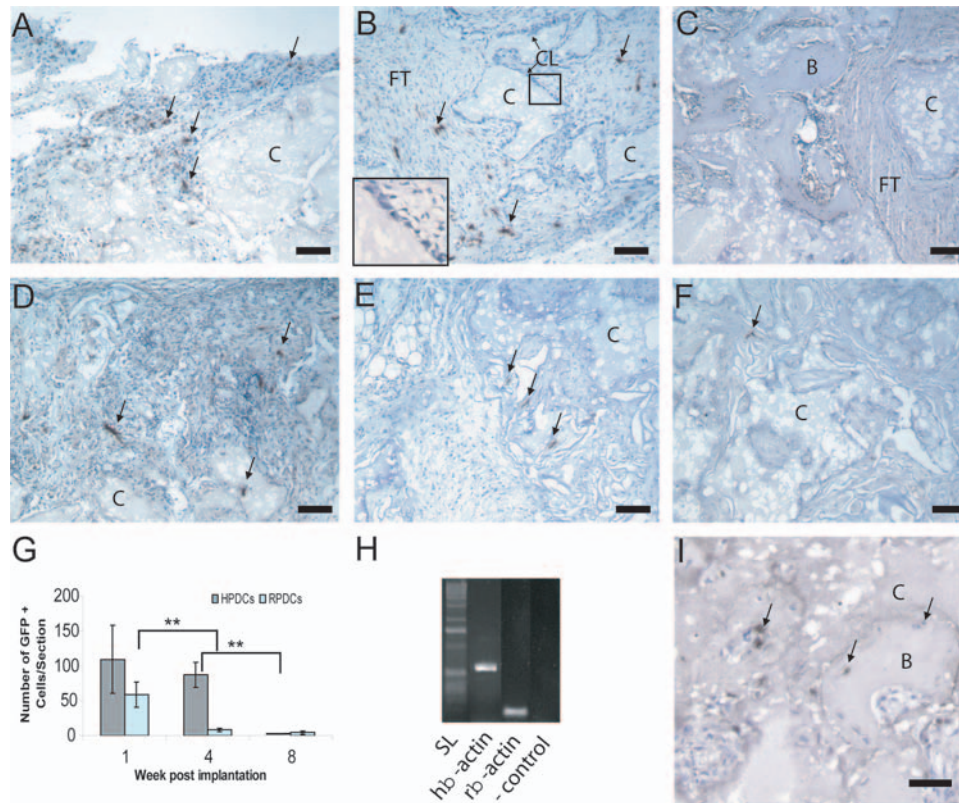


**FIG. 5.** Cell tracking using immunohistochemistry of ad-green fluorescent protein (GFP)-transduced human periosteum-derived cells (HPDCs) (A–C) and ad-GFP-transduced rabbit periosteum-derived cells (RPDCs) (D–F) in Collagraft at 1 week (A and D), 4 weeks (B and E), and 8 weeks (C and F) after implantation. The black arrows mark some of the GFP-positive cells. Notice the layer of cells surrounding the anorganic matrix of the Collagraft (Fig. 4B), which will give rise to newly formed bone (Fig. 4C) 8 weeks after implantation. A higher magnification (200 $\times$ ) of the cell layer is shown in Fig. 4B. (100 $\times$ , bar = 50 $\mu$ m; hematoxylin counterstained). (G) Quantification of GFP-positive cells per section. Each bar represents the average cell count of a least 15 sections of each implant. Error bars show the standard deviation (\*\* $p \leq 0.01$ ). (H) Conventional PCR of human-specific beta actin and rabbit beta actin in scaffolds seeded with HPDCs and RPDCs, respectively, after 8 weeks of implantation. (Water was used as negative control for both primer sets.) (I) Immunostaining against human-specific osteocalcin. The black arrows indicate some positive cells. B, bone; CL, cell layer; C, Collagraft; FT, fibrous tissue; h $\beta$ -actin, human-specific beta actin; r $\beta$ -actin, rabbit-specific beta actin; SL, step ladder. Color images available online at [www.liebertpub.com/ten](http://www.liebertpub.com/ten).

seeded HPDCs, were engrafted in the implants 4 weeks after implantation. A possible explanation for the difference in engraftment might be found in the metabolic activity of the 2 cell types. As indicated by the growth curves, RPDCs grew faster than HPDCs and thus may have a higher cellular metabolic activity. When RPDCs are seeded in Collagraft and implanted in nude mice, the microenvironment might initially not provide sufficient nutrients, and therefore fewer RPDCs than HPDCs can survive and engraft in the implant. The reduced cell viability of the non-adherent cells, as determined using the trypan blue exclusion test 24h after seeding, also suggested limited survival of the RPDCs. This needs to be interpreted with caution, because we do not know how well the cell viability of the non-adherent cells reflects the cell viability of the seeded cells in the scaffold. Alternatively, different population doublings (PDs) of the implanted cells might explain the differences between RPDCs and HPDCs. Based on the

growth curves, one would expect that P3 RPDCs have 4 more PDs than P3 HPDCs. To address this, we conducted osteogenic differentiation experiments *in vitro* and *in vivo* with P5 up to P10 HPDCs, and we did not notice any difference with the early passages (data not shown).

Some cells were positive for human osteocalcin, demonstrating that a subpopulation of the engrafted HPDCs contributed in a direct way to *de novo* bone formation. Also, others have published that implanted MSCs can contribute to ectopic bone formation in this model.<sup>2</sup> In addition, based on the observation that bone formation started at week 4 with GFP-positive HPDCs located in the fibrous tissue of the implant, we hypothesize that the implanted HPDCs may also exhibit a bone formation-stimulating paracrine function during the first 4 weeks after implantation.

In conclusion, we have demonstrated that periosteum-derived progenitor cells from humans and rabbits behave

differently in cell culture and *in vivo* in an ectopic bone-formation model under the culture conditions used. In this study, HPDCs but not RPDCs induced a cascade of events leading toward ectopic bone formation. Several other groups have demonstrated that RPDCs can form bone when implanted orthotopically.<sup>19,25,48</sup> Hence, it appears that the interaction between implant and microenvironment is an important one. Therefore it is necessary to understand the mode of action that drives the outcome of a tissue-engineered product in an animal model. Studying the interaction between a cell product and the microenvironment in at least 2 different species will lead to a better understanding of cell-based treatment and might be clinically relevant for human applications.

### ACKNOWLEDGMENTS

The authors would like to thank M. Marechal and J. Vanlauwe for harvesting rabbit and human periosteum. We are also grateful to A.D. Bakker for critical reading of the manuscript and to I. Derese, M. Daans, R. Lories, and P. Tylzanowski for technical advice. Finally, we would like to thank Dr. I. Martin for providing the macro to perform the histomorphometry. This work was supported by Katholieke Universiteit Leuven Grant IDO/00/006 and by Fonds voor Wetenschappelijk Onderzoek Grant G.0176.04.

### REFERENCES

- De Bari, C., Dell'Accio, F., Tylzanowski, P., and Luyten, F. P. Multipotent mesenchymal stem cells from adult human synovial membrane. *Arthritis Rheum.* **44**, 1928, 2001.
- Dell'Accio, F., De Bari, C., and Luyten, F. P. Microenvironment and phenotypic stability specify tissue formation by human articular cartilage-derived cells *in vivo*. *Exp. Cell Res.* **287**, 16, 2003.
- Qu-Petersen, Z. Q., Deasy, B., Jankowski, R., Ikezawa, M., Cummins, J., Pruchnic, R., Mytinger, J., Cao, B. H., Gates, C., Wernig, A., and Huard, J. Identification of a novel population of muscle stem cells in mice: potential for muscle regeneration. *J. Cell Biol.* **157**, 851, 2002.
- Pittenger, M. F., Mackay, A. M., Beck, S. C., Jaiswal, R. K., Douglas, R., Mosca, J. D., Moorman, M. A., Simonetti, D. W., Craig, S., and Marshak, D. R. Multilineage potential of adult human mesenchymal stem cells. *Science* **284**, 143, 1999.
- Bruder, S. P., Jaiswal, N., and Haynesworth, S. E. Growth kinetics, self-renewal, and the osteogenic potential of purified human mesenchymal stem cells during extensive subcultivation and following cryopreservation. *J. Cell Biochem.* **64**, 278, 1997.
- Cancedda, R., Mastrogiacomo, M., Bianchi, G., Derubeis, A., Muraglia, A., and Quarto, R. Bone marrow stromal cells and their use in regenerating bone. *Novartis Found. Symp.* **249**, 133, 2003.
- Dieudonne, S. C., Kerr, J. M., Xu, T., Sommer, B., DeRubeis, A. R., Kuznetsov, S. A., Kim, I. S., Ghebron, Robey P., and Young, M. F. Differential display of human marrow stromal cells reveals unique mRNA expression patterns in response to dexamethasone. *J. Cell Biochem.* **76**, 231, 1999.
- Satomura, K., Krebsbach, P., Bianco, P., and Ghebron, R. P. Osteogenic imprinting upstream of marrow stromal cell differentiation. *J. Cell Biochem.* **78**, 391, 2000.
- Ito, Y., Fitzsimmons, J. S., Sanyal, A., Mello, M. A., Mukherjee, N., and O'Driscoll, S. W. Localization of chondrocyte precursors in periosteum. *Osteoarthritis Cartilage* **9**, 215, 2001.
- Stafford, H. J., Roberts, M. T., Oni, O. O., Hay, J., and Gregg, P. Localisation of bone-forming cells during fracture healing by osteocalcin immunocytochemistry: an experimental study of the rabbit tibia. *J. Orthop. Res.* **12**, 29, 1994.
- Kojimoto, H., Yasui, N., Goto, T., Matsuda, S., and Shimomura, Y. Bone lengthening in rabbits by callus distraction. The role of periosteum and endosteum. *J. Bone Joint Surg. Br.* **70**, 543, 1988.
- De Bari, C., Dell'Accio, F., and Luyten, F. P. Human periosteum-derived cells maintain phenotypic stability and chondrogenic potential throughout expansion regardless of donor age. *Arthritis Rheum.* **44**, 85, 2001.
- Koshihara, Y., Hirano, M., Kawamura, M., Oda, H., and Higaki, S. Mineralization ability of cultured human osteoblast-like periosteal cells does not decline with aging. *J. Gerontol.* **46**, B201, 1991.
- Hutmacher, D. W. and Sittinger, M. Periosteal cells in bone tissue engineering. *Tissue Eng.* **9 Suppl 1**, S45, 2003.
- Nagamoto, N., Iyama, K., Kitaoka, M., Ninomiya, Y., Yoshioka, H., Mizuta, H., and Takagi, K. Rapid expression of collagen type X gene of non-hypertrophic chondrocytes in the grafted chick periosteum demonstrated by *in situ* hybridization. *J. Histochem. Cytochem.* **41**, 679, 1993.
- Nakahara, H., Goldberg, V. M., and Caplan, A. I. Culture-expanded human periosteal-derived cells exhibit osteochondral potential *in vivo*. *J. Orthop. Res.* **9**, 465, 1991.
- Nakahara, H., Bruder, S. P., Goldberg, V. M., and Caplan, A. I. *In vivo* osteochondrogenic potential of cultured cells derived from the periosteum. *Clin. Orthop. Res.* **259**, 223, 1990.
- Schantz, J. T., Hutmacher, D. W., Chim, H., Ng, K. W., Lim, T. C., and Teoh, S. H. Induction of ectopic bone formation by using human periosteal cells in combination with a novel scaffold technology. *Cell Transplant.* **11**, 125, 2002.
- Takushima, A., Kitano, Y., and Harii, K. Osteogenic potential of cultured periosteal cells in a distracted bone gap in rabbits. *J. Surg. Res.* **78**, 68, 1998.
- Jackson, D. W., Lalor, P. A., Aberman, H. M., and Simon, T. M. Spontaneous repair of full-thickness defects of articular cartilage in a goat model. A preliminary study. *J. Bone Joint Surg. Am.* **83-A**, 53, 2001.
- van Susante, J. L., Wymenga, A. B., and Buma, P. Potential healing benefit of an osteoperiosteal bone plug from the proximal tibia on a mosaicplasty donor-site defect in the knee. An experimental study in the goat. *Arch. Orthop. Trauma Surg.* **123**, 466, 2003.
- Wakitani, S. and Yamamoto, T. Response of the donor and recipient cells in mesenchymal cell transplantation to cartilage defect. *Microsc. Res. Tech.* **58**, 14, 2002.
- Wakitani, S., Goto, T., Pineda, S. J., Young, R. G., Mansour, J. M., Caplan, A. I., and Goldberg, V. M. Mesenchymal

- cell-based repair of large, full-thickness defects of articular cartilage. *J. Bone Joint Surg. Am.* **76**, 579, 1994.
24. Bo, B., Wang, C. Y., and Guo, X. M. [Repair of cranial defects with bone marrow derived mesenchymal stem cells and beta-TCP scaffold in rabbits]. *Zhongguo Xiu. Fu Chong. Jian. Wai Ke. Za Zhi.* **17**, 335, 2003.
  25. Breitbart, A. S., Grande, D. A., Kessler, R., Ryaby, J. T., Fitzsimmons, R. J., and Grant, R. T. Tissue engineered bone repair of calvarial defects using cultured periosteal cells. *Plast. Reconstr. Surg.* **101**, 567, 1998.
  26. Fialkov, J. A., Holy, C. E., Shoichet, M. S., and Davies, J. E. In vivo bone engineering in a rabbit femur. *J. Craniofac. Surg.* **14**, 324, 2003.
  27. Tsubota, S., Tsuchiya, H., Shinokawa, Y., Tomita, K., and Minato, H. Transplantation of osteoblast-like cells to the distracted callus in rabbits. *J. Bone Joint Surg. Br.* **81**, 125, 1999.
  28. Kuznetsov, S. A., Mankani, M. H., and Robey, P. G. Effect of serum on human bone marrow stromal cells: ex vivo expansion and in vivo bone formation. *Transplantation* **70**, 1780, 2000.
  29. Martin, I., Mastrogiacomo, M., De Leo, G., Muraglia, A., Beltrame, F., Cancedda, R., and Quarto, R. Fluorescence microscopy imaging of bone for automated histomorphometry. *Tissue Eng.* **8**, 847, 2002.
  30. Dell'Accio, F., De Bari, C., Neys, J., and Luyten, F. P. Multipotent cell populations from adult human articular cartilage. *Arthritis Rheum.* **44**, S61, 2001.
  31. Jaiswal, N., Haynesworth, S. E., Caplan, A. I., and Bruder, S. P. Osteogenic differentiation of purified, culture-expanded human mesenchymal stem cells in vitro. *J. Cell Biochem.* **64**, 295, 1997.
  32. Liu, F., Malaval, L., and Aubin, J. E. Global amplification polymerase chain reaction reveals novel transitional stages during osteoprogenitor differentiation. *J. Cell Sci.* **116**, 1787, 2003.
  33. Cheng, H., Jiang, W., Phillips, F. M., Haydon, R. C., Peng, Y., Zhou, L., Luu, H. H., An, N., Breyer, B., Vanichakarn, P., Szatkowski, J. P., Park, J. Y., and He, T. C. Osteogenic activity of the fourteen types of human bone morphogenetic proteins (BMPs). *J. Bone Joint Surg. Am.* **85-A**, 1544, 2003.
  34. Kang, Q., Sun, M. H., Cheng, H., Peng, Y., Montag, A. G., Deyrup, A. T., Jiang, W., Luu, H. H., Luo, J., Szatkowski, J. P., Vanichakarn, P., Park, J. Y., Li, Y., Haydon, R. C., and He, T. C. Characterization of the distinct orthotopic bone-forming activity of 14 BMPs using recombinant adenovirus-mediated gene delivery. *Gene Ther.* **11**, 1312, 2004.
  35. Chang, S. C., Chuang, H., Chen, Y. R., Yang, L. C., Chen, J. K., Mardini, S., Chung, H. Y., Lu, Y. L., Ma, W. C., Lou, J., Mardini, S., and Mardini, S. Cranial repair using BMP-2 gene engineered bone marrow stromal cells. *J. Surg. Res.* **119**, 85, 2004.
  36. Hicok, K. C., Du Laney, T. V., Zhou, Y. S., Halvorsen, Y. D., Hitt, D. C., Cooper, L. F., and Gimple, J. M. Human adipose-derived adult stem cells produce osteoid in vivo. *Tissue Eng.* **10**, 371, 2004.
  37. Perka, C., Schultz, O., Spitzer, R. S., Lindenhayn, K., Burmester, G. R., and Sittinger, M. Segmental bone repair by tissue-engineered periosteal cell transplants with bioresorbable fleece and fibrin scaffolds in rabbits. *Biomaterials* **21**, 1145, 2000.
  38. Schimming, R. and Schmelzeisen, R. Tissue-engineered bone for maxillary sinus augmentation. *J. Oral Maxillofac. Surg.* **62**, 724, 2004.
  39. Petropavlovskaja, M. and Rosenberg, L. Identification and characterization of small cells in the adult pancreas: potential progenitor cells? *Cell Tissue Res.* **310**, 51, 2002.
  40. Sekiya, I., Larson, B. L., Smith, J. R., Pochampally, R., Cui, J. G., and Prockop, D. J. Expansion of human adult stem cells from bone marrow stroma: conditions that maximize the yields of early progenitors and evaluate their quality. *Stem Cells* **20**, 530, 2002.
  41. Prockop, D. J., Sekiya, I., and Colter, D. C. Isolation and characterization of rapidly self-renewing stem cells from cultures of human marrow stromal cells. *Cytotherapy* **3**, 393, 2001.
  42. Youn, I., Suh, J. K., Nauman, E. A., and Jones, D. G. Differential phenotypic characteristics of heterogeneous cell population in the rabbit periosteum. *Acta Orthop.* **76**, 442, 2005.
  43. Hung, S. C., Chen, N. J., Hsieh, S. L., Li, H., Ma, H. L., and Lo, W. H. Isolation and characterization of size-sieved stem cells from human bone marrow. *Stem Cells* **20**, 249, 2002.
  44. Bodger, M. P., Hann, I. M., Maclean, R. F., and Beard, M. E. Enrichment of pluripotent hemopoietic progenitor cells from human bone marrow. *Blood* **64**, 774, 1984.
  45. Conlon, I. and Raff, M. Size control in animal development. *Cell* **96**, 235, 1999.
  46. Sugiura, F., Kitoh, H., and Ishiguro, N. Osteogenic potential of rat mesenchymal stem cells after several passages. *Biochem. Biophys. Res. Commun.* **316**, 233, 2004.
  47. Kim, H., Lee, J. H., and Suh, H. Interaction of mesenchymal stem cells and osteoblasts for in vitro osteogenesis. *Yonsei Med. J.* **44**, 187, 2003.
  48. Kadiyala, S., Young, R. G., Thiede, M. A., and Bruder, S. P. Culture expanded canine mesenchymal stem cells possess osteochondrogenic potential in vivo and in vitro. *Cell Transplant.* **6**, 125, 1997.
  49. Solchaga, L. A., Cassiede, P., and Caplan, A. I. Different response to osteo-inductive agents in bone marrow- and periosteum-derived cell preparations. *Acta Orthop. Scand.* **69**, 426, 1998.
  50. Tenenbaum, H. C. and Heersche, J. N. Dexamethasone stimulates osteogenesis in chick periosteum in vitro. *Endocrinology* **117**, 2211, 1985.
  51. Liu, Y., Titus, L., Barghouthi, M., Viggswarapu, M., Hair, G., and Boden, S. D. Glucocorticoid regulation of human BMP-6 transcription. *Bone* **35**, 673, 2004.
  52. Diefenderfer, D. L., Osyczka, A. M., Reilly, G. C., and Leboy, P. S. BMP responsiveness in human mesenchymal stem cells. *Connect. Tissue Res.* **44 Suppl 1**, 305, 2003.
  53. Osyczka, A. M., Diefenderfer, D. L., Bhargava, G., and Leboy, P. S. Different effects of BMP-2 on marrow stromal cells from human and rat bone. *Cells Tissues Organs* **176**, 109, 2004.
  54. Osyczka, A. M. and Leboy, P. S. Regulatory kinases in BMP-2 induced human MSC osteogenesis. 5th International Conference on Bone Morphogenetic Proteins, Nagoya, JAPAN 125, 2004.
  55. Nakahara, H., Goldberg, V. M., and Caplan, A. I. Culture-expanded periosteal-derived cells exhibit osteochondrogenic potential in porous calcium phosphate ceramics in vivo. *Clin. Orthop.* **291**, 1992.

56. Katz, R. W., Felthousen, G. C., and Reddi, A. H. Radiation-sterilized insoluble collagenous bone matrix is a functional carrier of osteogenin for bone induction. *Calcif. Tissue Int.* **47**, 183, 1990.
57. Ripamonti, U., Van Den, H. B., Sampath, T. K., Tucker, M. M., Rueger, D. C., and Reddi, A. H. Complete regeneration of bone in the baboon by recombinant human osteogenic protein-1 (hOP-1, bone morphogenetic protein-7). *Growth Factors* **13**, 273, 1996.
58. Akahane, M., Ohgushi, H., Kuriyama, S., Akahane, T., and Takakura, Y. Hydroxyapatite ceramics as a carrier of gene-transduced bone marrow cells. *J. Orthop. Sci.* **7**, 677, 2002.

Address reprint requests to:

*Frank P. Luyten, M.D., Ph.D.*

*Lab for Skeletal Development and Joint Disorders*

*Onderwijs en Navorsing 8<sup>th</sup> floor, bus 813*

*3000 Leuven, Belgium*

*E-mail: Frank.Luyten@uz.kuleuven.be*

